DEPARTMENT OF THE INTERIOR

U.S. GEOLOGICAL SURVEY

Acoustic Evidence for Gas-Charged Sediment in the Abyssal Aleutian Basin, Bering Sea, Alaska

by

Douglas M. Rearic[1], Stephen R. Williams[2], Paul R. Carlson[1], and Robert K. Hall[1]

Open-File Report 88-677

---

[1] U.S. Geological Survey, Menlo Park, California

[2] Formerly of Institute of Oceanographic Sciences, Wormley, United Kingdom; Now at British Petroleum Oil Co., London, United Kingdom

INTRODUCTION

The U.S. Geological Survey and the U.K. Institute of Oceanographic Sciences recorded seismic-reflection profiles across the Aleutian Basin during a survey of part of the Bering Sea in July 1986 (fig. 1; Carlson et al., 1987). This survey (F2-86-BS) was part of a larger survey of the USA Exclusive Economic Zone (Rowland et al., 1983). The main objective of the cruise was the imaging of the sea floor with GLORIA (Geological Long-Range Inclined Asdic) side-scanning sonar, however geophysical and geopotential data also were collected. In order to obtain seismic reflection profiles, a 160 in^3 airgun source was used and two-channel seismic reflection data were recorded in analogue format on an EPC[3] graphic recorder. The tracklines were oriented 123°T-303°T with a constant line spacing of about 30 km in the basin. A total of about 9800 km of trackline were surveyed with the two-channel airgun during cruise F2-86-BS. Other data acquired during the survey included 3.5 kHz seismic reflection profiles, 10 kHz echo soundings, and gravity and magnetic measurements.

The data were collected in a part of the Aleutian Basin where VAMPs had previously been detected (Scholl and Cooper, 1978). The regular survey pattern facilitates a quantitative evaluation of the distribution of VAMPs. However, the directional bias in the survey pattern affects the probability of detecting linear features with orientations parallel to the tracklines. The wide spacing of the tracks also limits determination of the configuration of individual VAMPs.

---

[3] Any use of trade names does not imply endorsement by the United States government.

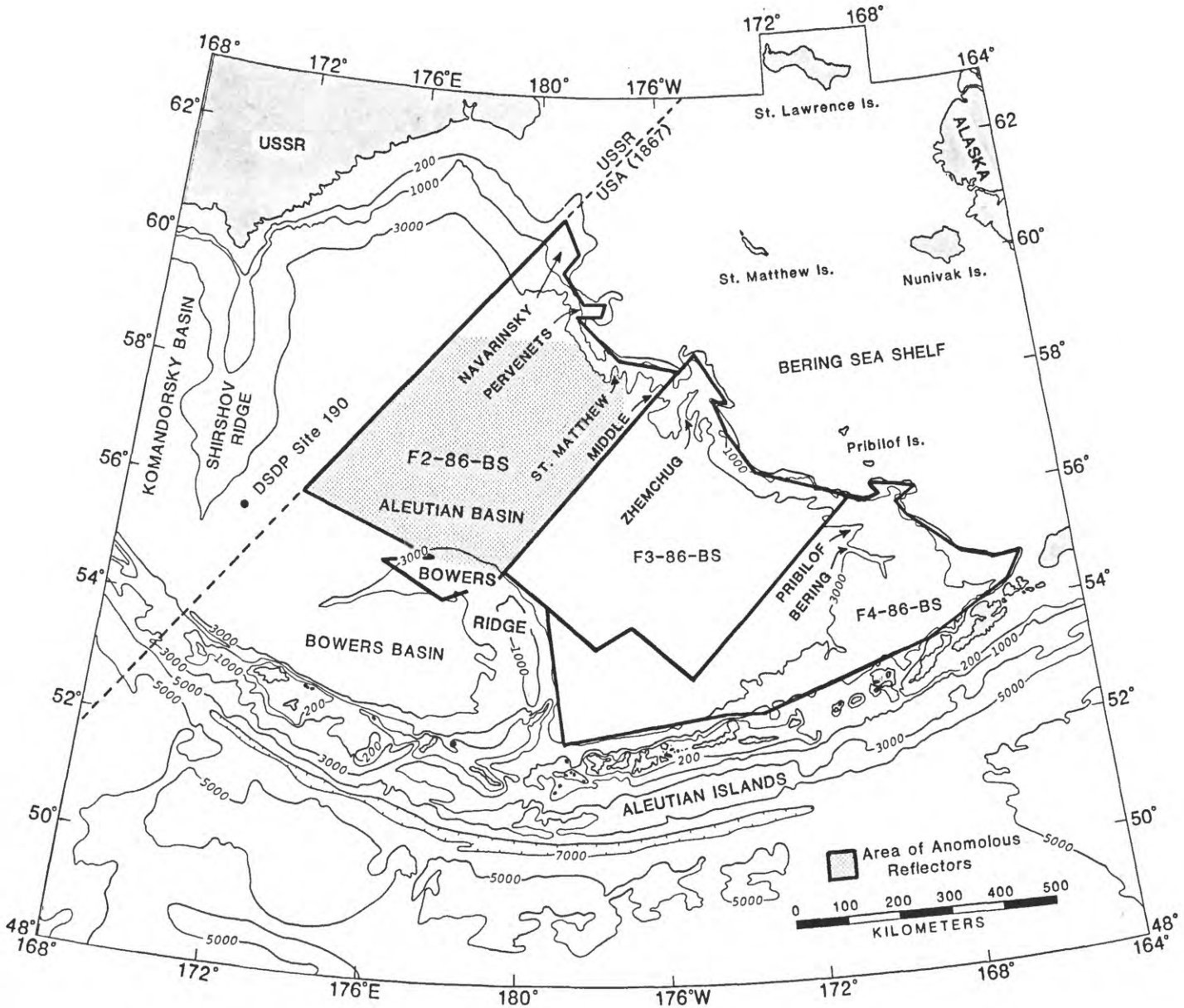

Figure 1. Map of the study area showing the GLORIA EEZ cruises of 1986. Stippled area of cruise F2-86-BS represents the area of figure 2 and the general area in which the acoustic anomalies were recorded.

The term VAMP (Velocity-AMPlitude feature) was coined by Scholl and Cooper (1978) to describe features observed on seismic-reflection profiles from the Aleutian Basin in the Bering Sea. They defined VAMPs as "time-based recordings of a narrow subsurface column of concave reflection horizons that commonly are associated with an overlying highly reflective horizon". VAMPs may indicate accumulations of gaseous hydrocarbons, which may become economically attractive in the future. In this report we discuss the results of the seismic survey, describe a quantitative study of VAMPs observed in the same area (fig. 2), and compare these results with those of Scholl and Cooper (1978).

Geologic Setting

The Aleutian Basin (fig. 3A and 3B) lies within the Bering Sea basin, a marginal basin which was separated from the Pacific Ocean by growth of the Aleutian Ridge in the Eocene. Two smaller interior ridges, Bowers and Shirsov Ridges, formed at or after this time and separate the Aleutian Basin from Bowers Basin in the south and Komandorsky Basin in the west. The northern and eastern boundaries of the Aleutian Basin are bordered by the Beringian shelf and slope. The bathymetry of the Aleutian Basin (fig. 2; Hall et al., in press) shows that there is a gentle sloping of the basin to the south. Since the middle Eocene, pelagic and terrigenous sediment has infilled the basin to a thickness of about 2-9 km (fig. 4; Marlow et al., 1979). The Aleutian Basin is underlain by a thick sequence of sediment overlying oceanic basement of probable Early Cretaceous age. The depth to acoustic basement was interpreted by Cooper et al. (1979b) (fig. 5). A series of en echelon basement ridges (fig. 2) extends throughout

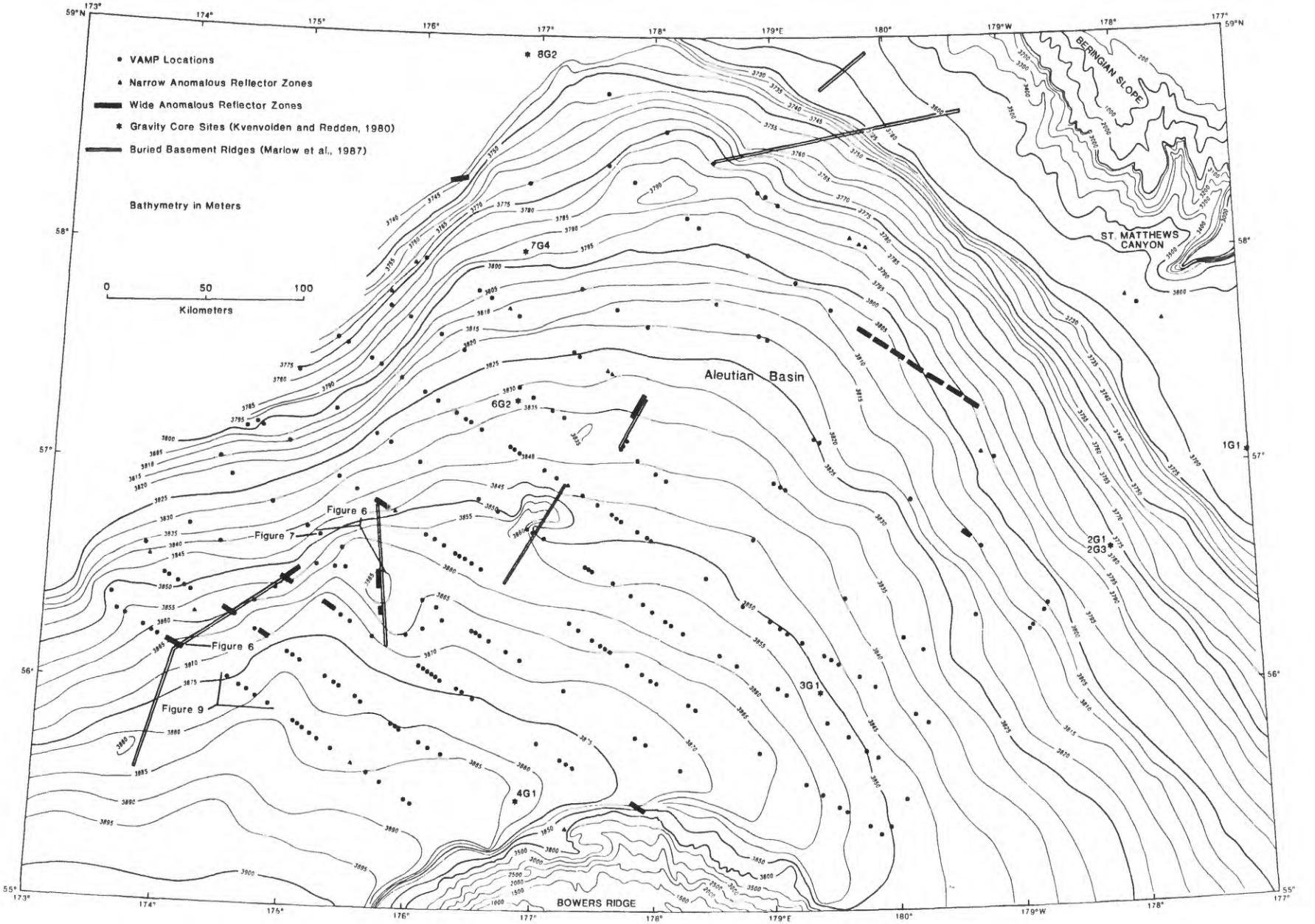

Figure 2. Bathymetry map of the area of acoustic anomalies. Note the increase in number of anomalies from north to south.

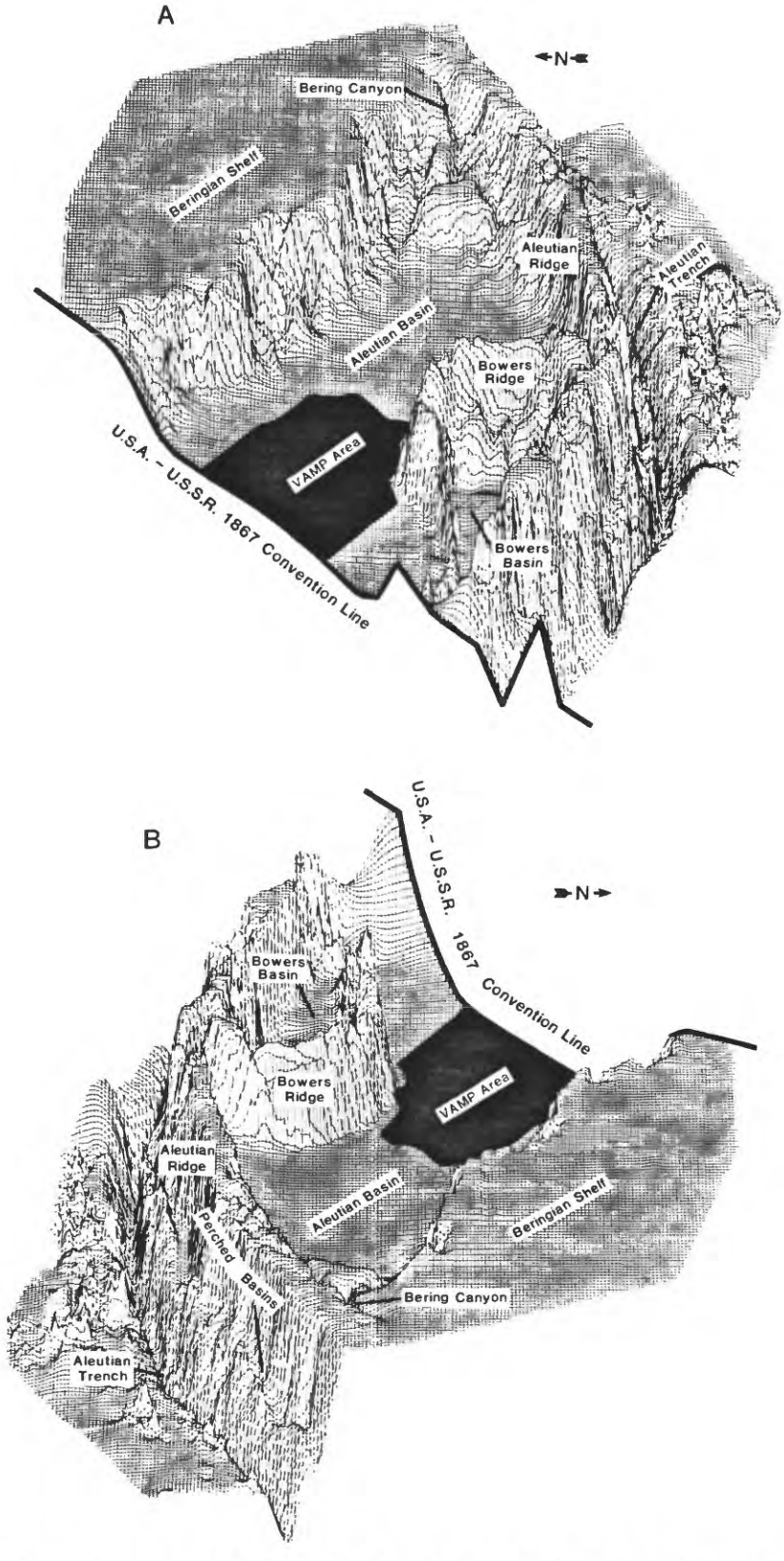

Figure 3. Three-dimensional perspective of the Aleutian Basin showing many of the features of the basin and surrounding margins and their geographical relation to each other. Figure 3A is a view to the east and figure 3B is a view to the west. Vertical exaggeration is about 100:1.

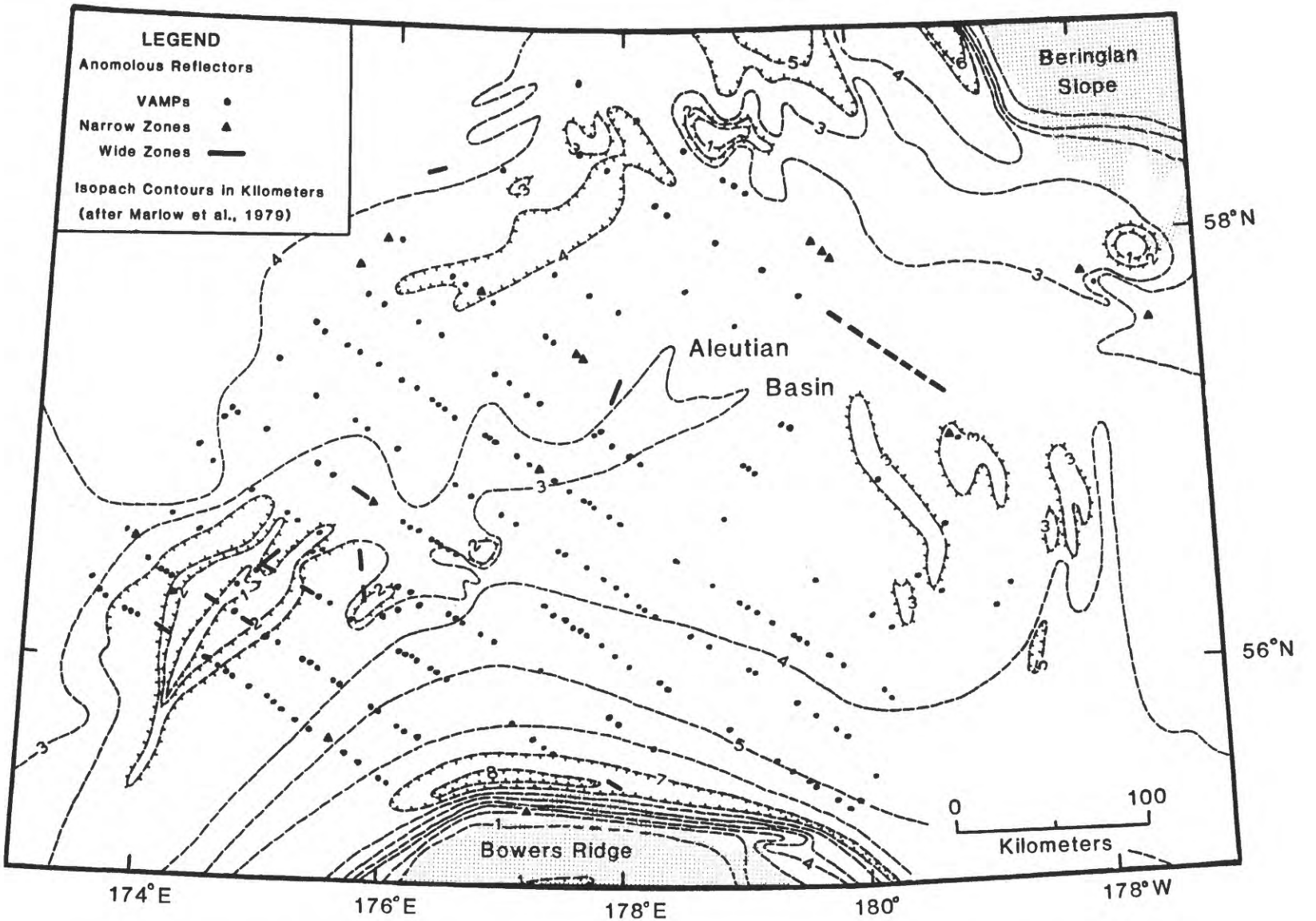

Figure 4. Isopach map of sediment thickness in the central Aleutian Basin. Note the general increase in thickness from north to south. Stippled area represents depths shallower than 3500 m.

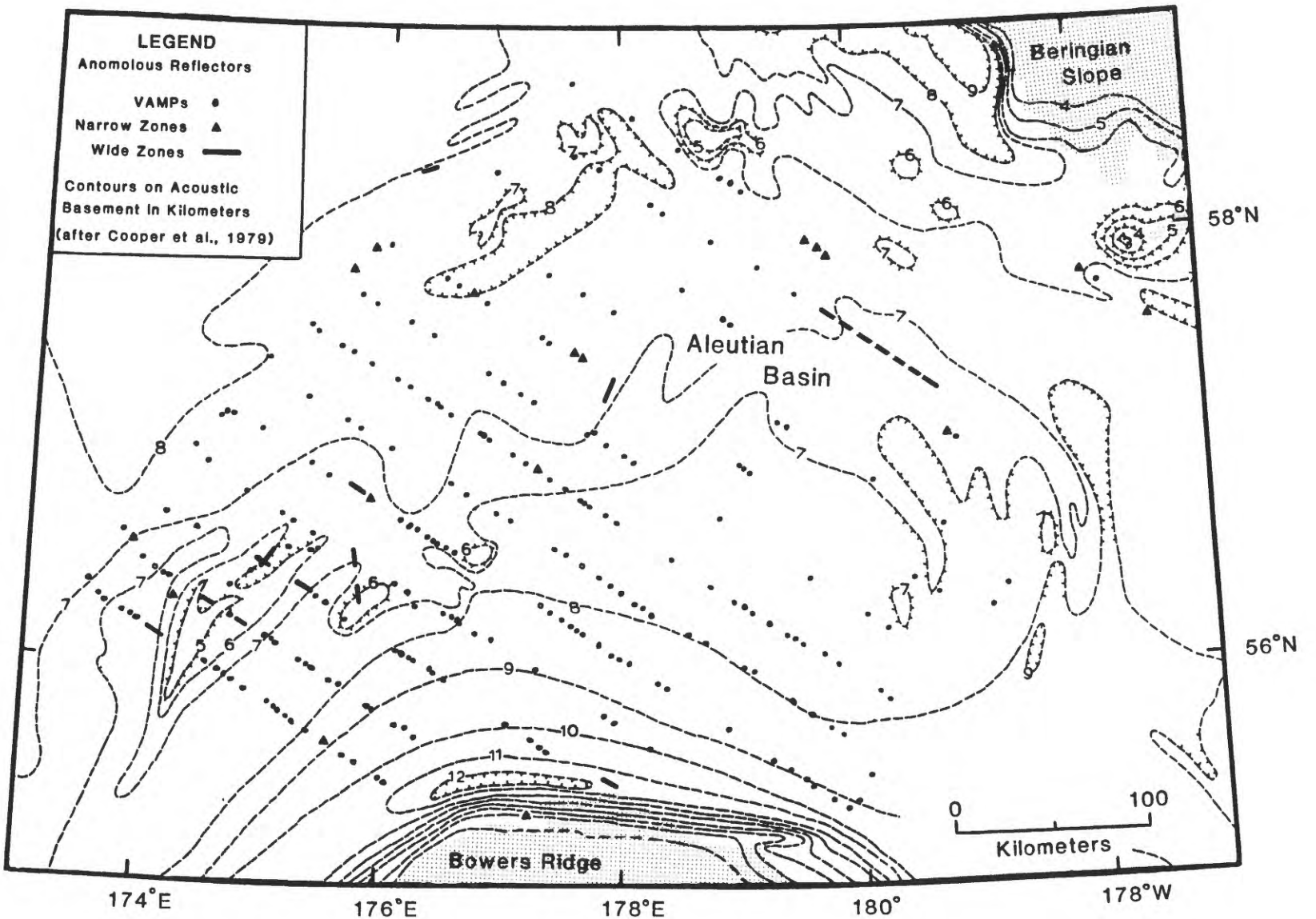

Figure 5. Map of depth to acoustic basement in the central Aleutian Basin. Note the general increase in basement depth from north to south, similar to the increase noted in figure 4. Stippled area represents depths shallower than 3500 m.

the basin and, locally, may rise to within 600 m of the sea floor (Marlow et al., 1987).

The stratigraphy of the basin sediment can be extrapolated from DSDP site 190 (Creager et al., 1973) which lies west of the VAMP area. This hole was drilled to a sub-bottom depth of 627 m in a total sediment column of 1100 m. Unit A (0-615 m) consists of two sections. The uppermost 375 m is described as Pleistocene and upper Pliocene diatom-rich silty clay interbedded with terrigenous turbidites. Semi-indurated diatom-rich silty clay is found between 375 m and 615 m. The diatomaceous beds of the lower section are porous (58-85 %) and permeable (10-35 md) (Cooper et al., 1979b). Unit B (between 615 m and the bottom of the hole at 627 m, but of unknown thickness) is a highly-indurated mudstone with possible thin carbonate beds. A similar sequence is expected in the area of the VAMPs although sequence thicknesses should be proportionately greater because DSDP site 190 was drilled through a condensed sediment sequence overlying a basement knoll. Velocities within the upper 425 m of diatomaceous sediment range between 1.5 and 1.6 km/sec (Creager et al., 1973). Velocities were not obtained for sediment deeper than 425 m.

Characteristics of VAMPs

The distribution, size and type of seismic anomalies associated with VAMPs are detailed in figure 2 and appendices 1 and 2. The essential attribute of a VAMP, as defined by Scholl and Cooper (1978), is a narrow (1-2 km wide) column of concave upward reflectors on a time-based profile (figs. 6 and 7). This geometry is attributed to velocity pulldown caused by localized low-velocity material. The recognition of pull-down is dependent on the vertical exaggeration of the profiles. Vertical exaggeration

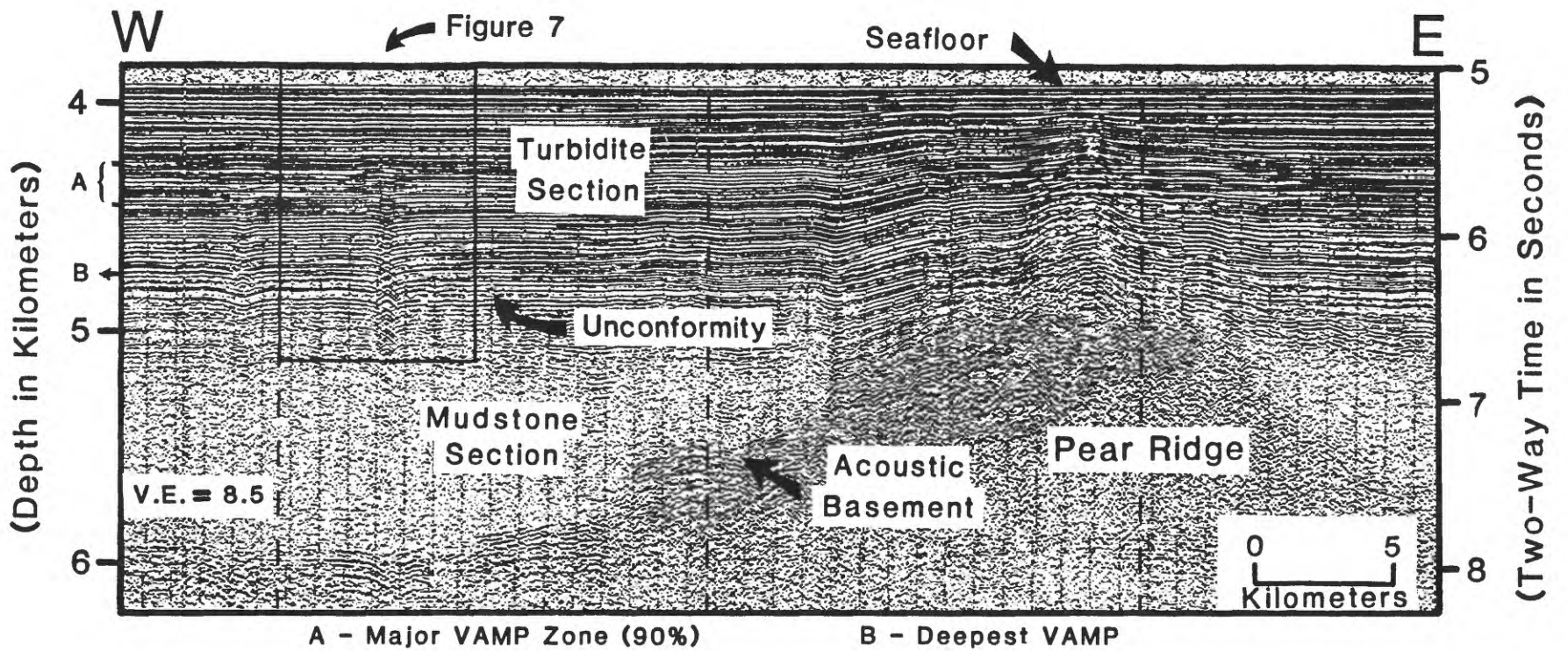

Figure 6. Airgun record (160 cu. in.) of a section of sea floor covering Pear Ridge (Marlow et al., 1986). Note the difference in the acoustic signature between the upper turbidite section and the lower mudstone section. See figure 2 for location.

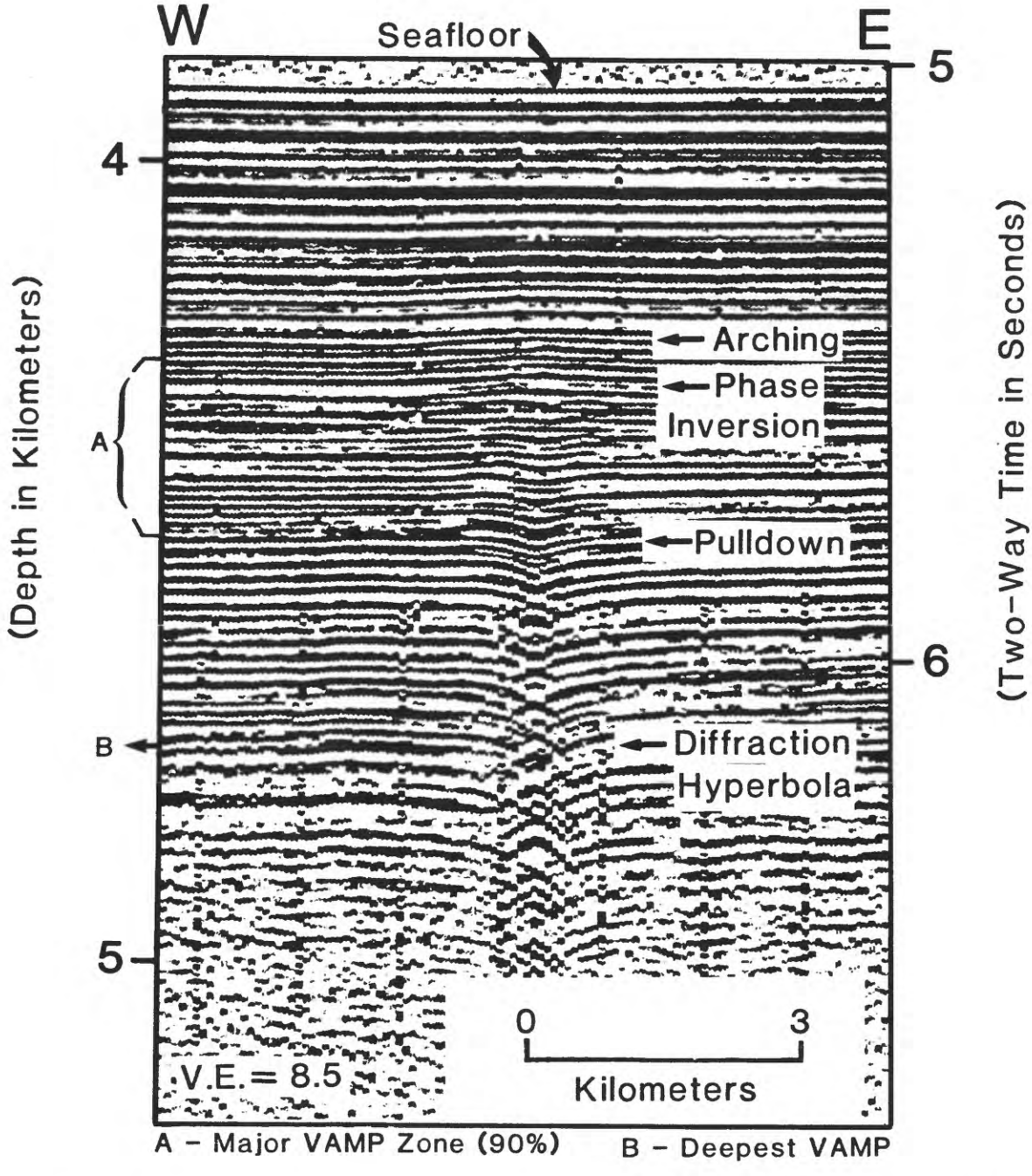

Figure 7. Expanded airgun record (160 cu. in.) of a VAMP exhibiting many of the characteristics generally associated with VAMPs. See figures 2 and 6 for location.

of the seismic records from this study ranges from 7 to 8.5 and we estimate that we could resolve deflections in the seismic reflectors of about 10 msec.

Phase inversion of overlying reflectors is commonly associated with VAMPs. Phase inversion is caused by reflection at a boundary where the acoustic impedance (density x velocity) decreases or increases relative to the acoustic impedance of the overlying sediment. Velocity and density changes may be caused by changes in lithology, cementation, porosity, or pore-fluid composition. Apparent phase inversion may also be caused by interference and such occurrences were eliminated from consideration. Figure 7 shows an example of phase inversion associated with a VAMP.

Gentle arching commonly affects the reflectors overlying a pulldown zone (fig. 7). The convex upwards reflectors have been attributed to a decrease in the acoustic impedance between upper and lower beds as a result of gas hydrate in the sediment (Scholl and Cooper, 1978). Arching may also be an indication of basement relief and differential compaction of the overlying sediment (Cooper et al., 1979b).

High-amplitude reflectors commonly occur at about the same depth as phase inversion. High-amplitude reflectors may be attributed to strong impedance contrasts at the top of a low-impedance zone. Apparent high-amplitude reflectors may be caused by interference and, again, care was taken to exclude such occurrences from our interpretations. It was not possible to quantify the intensity of the high-amplitude reflectors.

Diffraction hyperbola and bow-tie structures are seismic artifacts produced by discontinuities of structure, lithology, or impedance. They occur commonly in VAMPs

(fig. 7).

The topography of the underlying basement may influence the genesis of a VAMP. Scholl and Cooper (1978) reported that VAMPs are commonly seen overlying basement highs. We, therefore, made note of the basement topography associated with each VAMP where possible (Appendix 1).

Quantitative Analysis

We measured the following VAMP characteristics: width; depth to the shallowest occurrence of phase inversion or high-amplitude reflector, or failing that, depth to the shallowest occurrence of reflector pulldown; depth to the shallowest occurrence of arching; and topography of the underlying basement (high, low, flat, or dipping). The basement categorization was somewhat subjective due to the varying wavelength and amplitude of the basement relief. We considered relief with a wavelength less than 10 km and an amplitude greater than 200 msec to be basement highs. We then calculated basic statistics from the data (Table 1) as well as the frequency of the characteristics listed above (Tables 2 and 3).

Where the profiles cross large basement ridges (Marlow et al., 1987) it becomes difficult to isolate VAMPs from a confused background of features such as interference, pinchouts, and faults. We studied the reflector patterns over crossings of the larger basement ridges and we recorded the following observations: whether the reflectors were conformable and continuous or discontinuous over the high (figs. 6 and 8); whether the basement reflector was well-defined; whether features such as diffraction hyperbola, bright spots, flat spots, and side-swipe or pulldown were present.

Table 1. VAMP Statistics.

VAMP Attribute	Range	Mean	St. Deviation
Width (km)	0.50-3.75	1.30	0.45
Depth to P.I. or pulldown (msec)	450-1100	609.3	129.2
Max. Amplitude of pulldown (msec)	10-70	23.3	11.7
Depth to Arching	100-800	364.4	104.2

Table 2. Characteristics of Aleutian Basin VAMPS.

Reflector Anomaly	% Occurence
Pulldown	100
Phase Inversion	78
Arching Reflectors	58
Diffraction Hyperbola	21
High Amplitude Reflector	18

Table 3. VAMP Basement Morphology.

Basement Type	% Occurence
Flat	53
Dipping and Arched	28
Depressed	4
Unknown	15

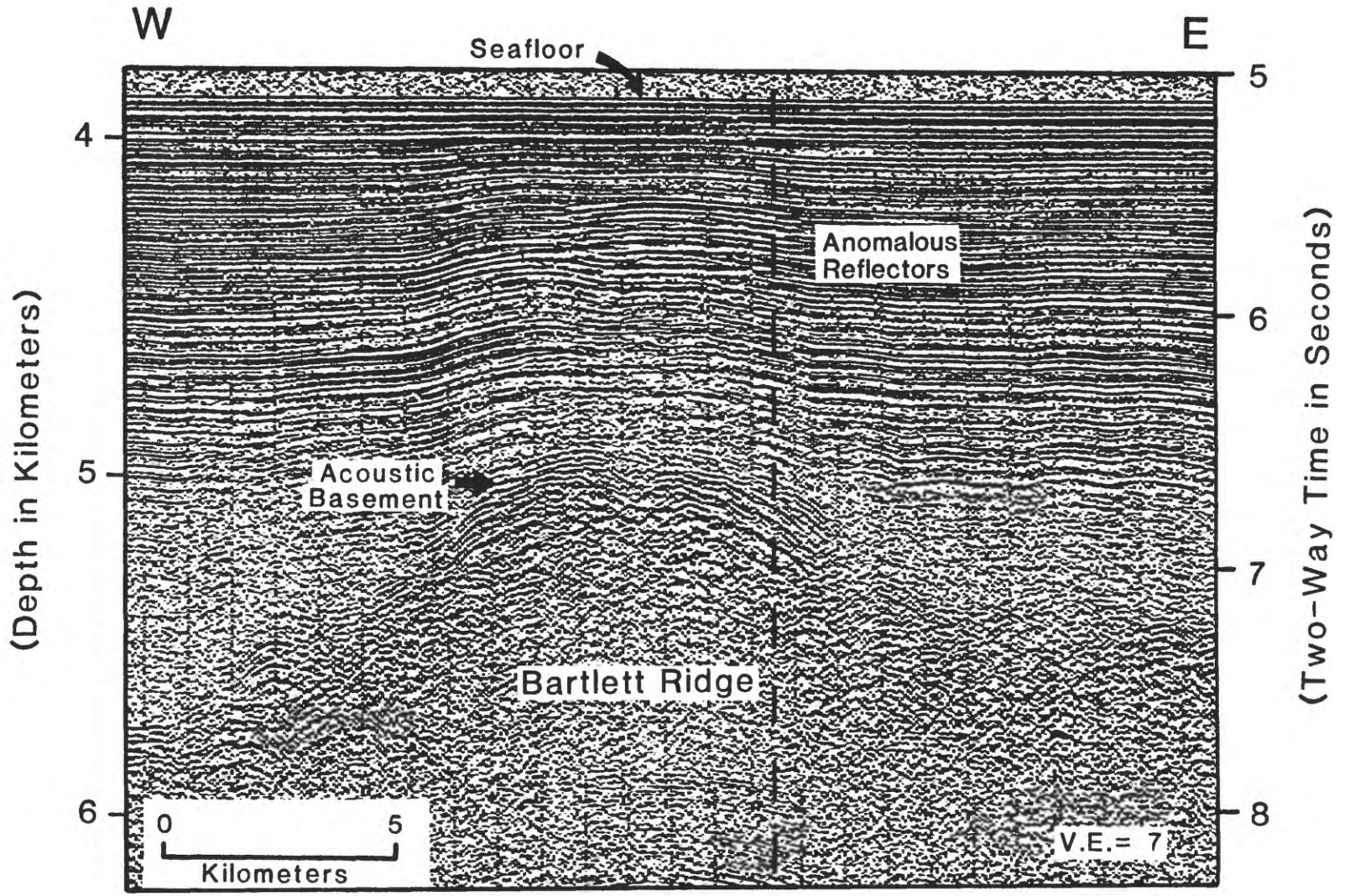

Figure 8. Airgun record (160 cu. in.) of Bartlett Ridge. Note the bright spots and discontinuous reflectors over the crest of the ridge. The convex reflectors over the ridge are attributed to differential compaction and faulting (Marlow et al., 1987). See figure 2 for location.

Other anomalous features were observed which displayed no pulldown but did display other attributes associated with VAMPs. These are divided into wide (Appendix 2) and narrow anomalous reflector zones (fig. 2). We noted such occurrences but excluded them from our statistics.

RESULTS

In this report we describe 277 anomalous features which are clearly present on our reflection profiles. Of this number, 246 are described as VAMPS, 14 as wide anomalous reflector zones, and 17 as narrow anomalous reflector zones.

Distribution

The VAMPs from this study fall within the geographical limits previously designated by Scholl and Cooper (1978) and Cooper et al. (1979b) (fig. 2). The regular pattern of our survey does, however, give a better indication of the areal distribution of the VAMPs. The most significant pattern is the increase in density toward the south of the basin, approaching the fossil island arc of Bowers Ridge. This coincides with a general increase in depth to basement and sediment thickness in the basin (Cooper et al., 1979a; Marlow et al., 1979). The VAMPs found in the southern Aleutian Basin are also more closely spaced (fig. 9) compared to those found in the northern part of the basin (fig. 2).

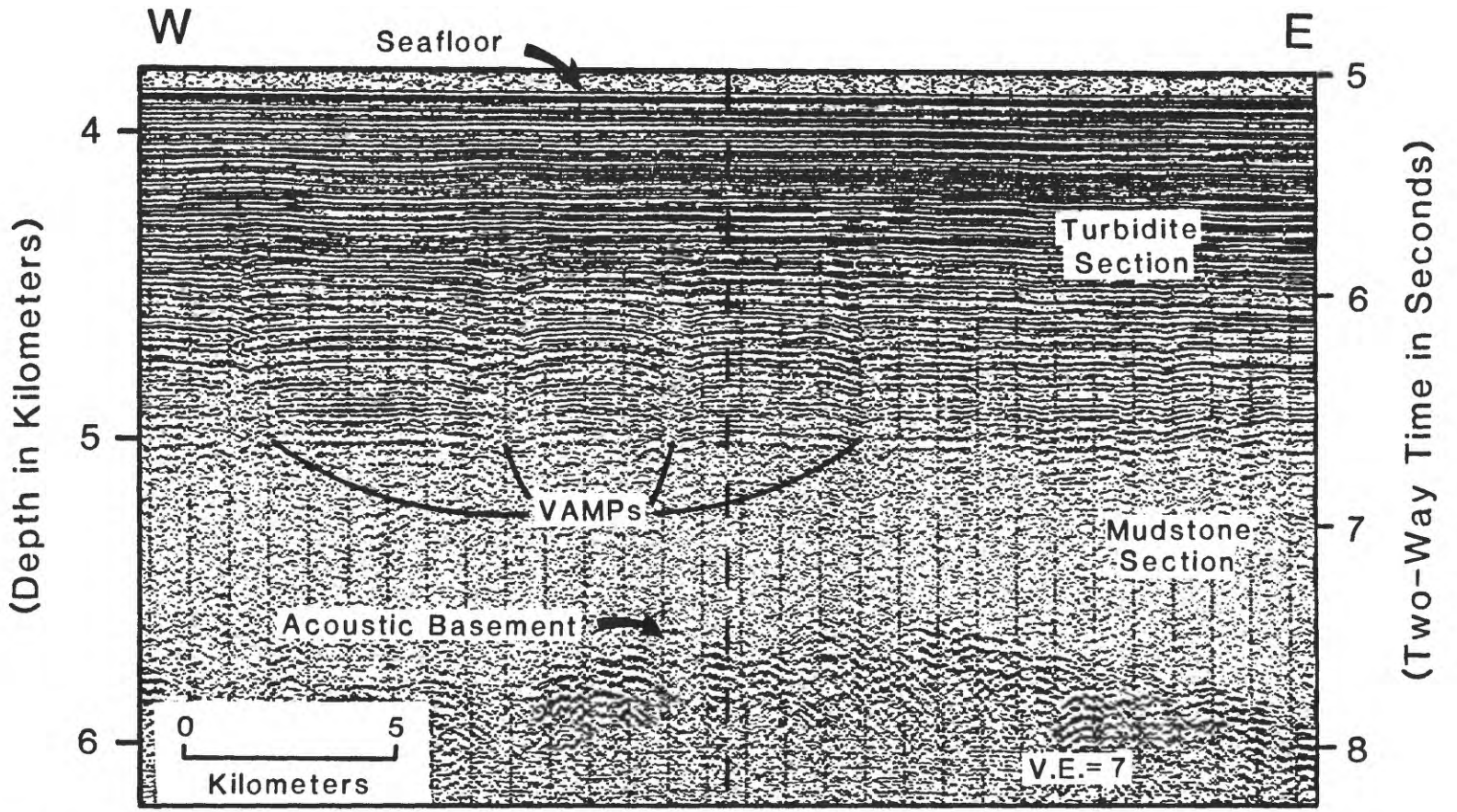

Figure 9. Airgun record (160 cu. in.) of an area of closely spaced VAMPs. The VAMPs occur over a slight basement high, begin in the diatomaceous-turbidite section, and extend downward into the mudstone section. See figure 2 for location.

Depth to Pulldown

VAMPs in the Aleutian Basin are found between sub-sea floor depths of 450 and 1100 msec. However, about 90 % of the VAMPs profiled in this study are between 450 and 750 msec deep (fig. 10). Average depth to pulldown is 609 msec with a standard deviation of 129 msec (Table 1).

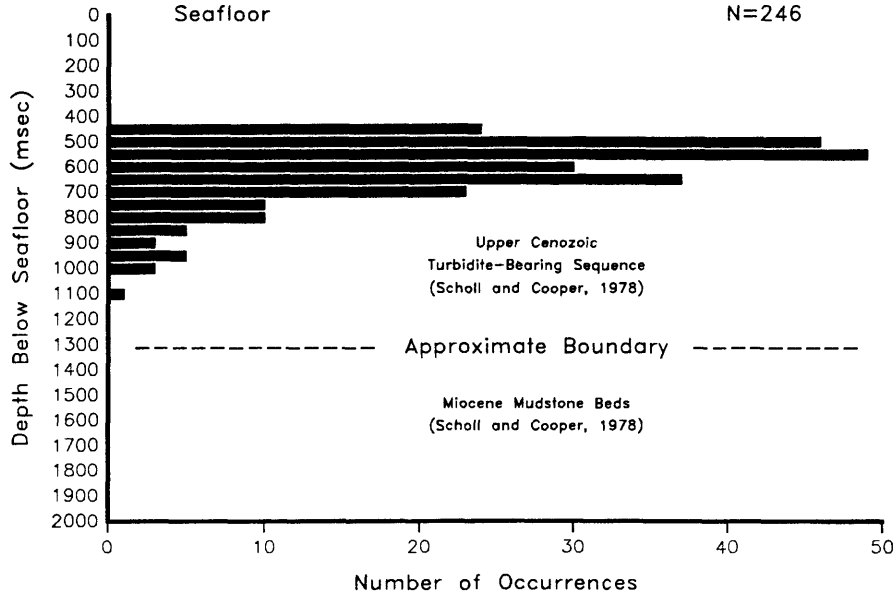

Figure 10. Graph of VAMP depth frequency. Note the 450 msec boundary and the drop-off frequency with depth downsection. The depths represent the first occurrence of phase inversion, high-amplitude reflector, or pulldown. Also note the approximate depth of the boundary between the upper diatomaceous-turbidite section and the lower mudstone section.

From the work of Scholl and Cooper (1978), analysis of data from DSDP Site 190 (Scholl and Creager, 1973), and interpretation of seismic reflection data from the present study, VAMPs seem to be restricted to sediment previously described as an

upper Cenozoic diatomaceous silty-clay sequence. Some anomalies, in particular pull-downs and diffraction hyperbola, extend into the underlying sediment below an unconformity separating the upper Cenozoic (<2.5 m.y.) turbidite-bearing diatomaceous sequence from Miocene (?) mudstone beds. The unconformity in the mid-Aleutian Basin lies at a sub-sea floor depth of about 1300 msec (fig. 7).

Pulldown Amplitude

The amplitude of the pulldowns ranges from 10 to 70 msec and averages 23 msec with a standard deviation of about 12 msec (Table 1). The amplitude of the pulldown generally increases with depth suggesting that if the feature is gas-charged sediment the gas may extend through the unconformity into the underlying Miocene (?) mudstone.

Width

VAMPs range between 0.5- and 3.75-km wide across the interval of pulldown (figs. 6 and 7). Mean width is 1.3 km with a standard deviation of 0.5 km (Table 1). This agrees favorably with the 1- to 2-km width reported by Scholl and Cooper (1978). Other anomalous reflector zones may be narrow (the width of a VAMP) or wide (up to 15 km). These zones do not demonstrate any pulldown of the reflectors, but do contain one or more of the other characteristics associated with VAMPs. Many of the wide zones are found over buried basement-ridge crests (Marlow et al., 1987; fig. 2 and 8).

Because of the consistent trackline orientation necessary for mosaicking the GLORIA imagery only 5% (11) of the VAMPs were profiled in an orientation normal to the other 95% of the VAMPs. These VAMPs ranged in width from 1.00 to 2.00 km and had a mean width of 1.45 km with a standard deviation of 0.29 km, very similar to the statistics of all the VAMPs from this study.

Phase Inversion and High-Amplitude Reflectors

After pulldown, phase inversion is the most common attribute of VAMPs. Phase-inverted reflectors (fig. 7 and Table 2) were observed in 78% of the VAMPs. High-amplitude reflectors were associated with 12% of the VAMPS. Both phase inversion and high-amplitude reflectors occur at or near the top of VAMPS and also are associated with other anomalous reflector zones lacking pulldowns.

Arching of Overlying Reflectors

Over half of the VAMPs surveyed (58%) had arching of the associated overlying reflectors (fig. 7). The arched reflectors are generally continuous features and do not display any of the anomalous characteristics normally associated with VAMPs (i.e. phase inversion, high-amplitude reflectors, etc.). Arching tends to decrease in an upward direction but could be detected at the sea bed in some areas with as much as 2 m of bathymetric relief detected on precision echo soundings. The average sub-sea floor depth at which arching is first detected is 364 msec with a standard deviation of 104 msec (Table 1). The thickness of the arched reflector section increases with increasing VAMP depth (fig. 11).

Diffraction Hyperbola

Diffraction hyperbola and bow-tie structures are features associated with 21% of the VAMPs (figs. 6 and 7; Table 2). Diffractions on reflection profiles are usually caused by structural discontinuities such as faults or steeply dipping interfaces. Such structures are rare within the turbidite sequence and thus these features are attributed to lateral variations in seismic velocity which cause disruption to seismic ray-paths.

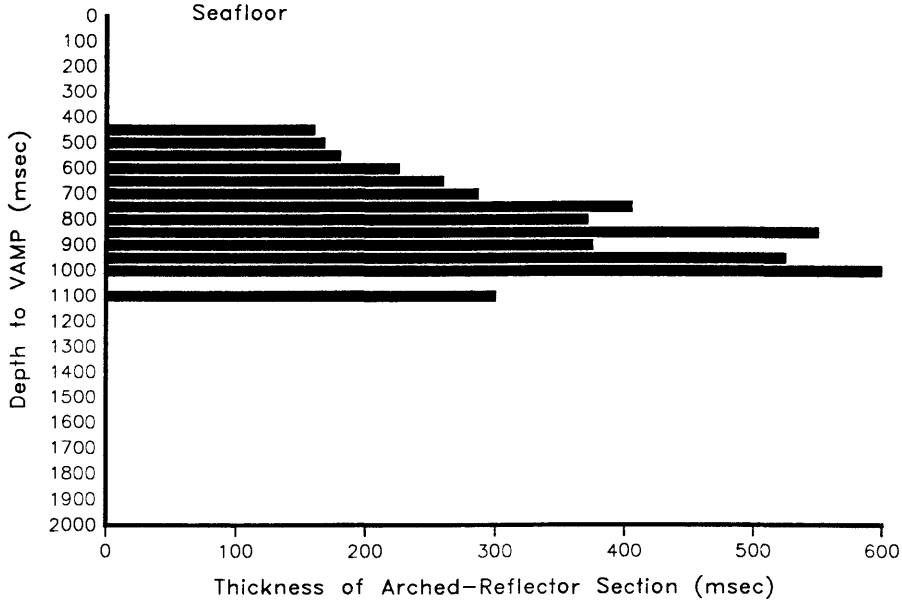

Figure 11. Graph of arched-reflector thickness verses VAMP depth. Note the thickness increase with VAMP depth.

Basement Topography

Scholl and Cooper (1978) report that most VAMPs are associated with basement highs. However, in the present survey only 28% of the VAMPS occur over basement

highs, whereas 57% occur over flat or depressed basement (Table 3). In about 15% of the cases, the basement was unresolvable beneath the VAMP.

Attribute Correlations

Attempts to correlate Vamp attributes were unsuccessful and, therefore, VAMP attributes appear to be independent of each other. Isopach maps of VAMP depth, width, and amplitude, as well as depth to arching were attempted, also, with unsuccessful results. The lack of correlation and regularity between attributes and distributions seems to suggest that VAMPs are independent features controlled only by the properties of the host sediment.

DISCUSSION

Acoustic Anomalies

Our 1986 survey confirms some of the conclusions of Scholl and Cooper (1978), fails to confirm other conclusions, and adds to the general body of knowledge concerning VAMPs and other acoustic anomalies in the Aleutian Basin. Our measurements of VAMP characteristics show that VAMPs are found in a very restricted depth range with 90 percent occurring between 450-750 msec (fig. 10). Using the minimum average velocity of 1500 m/sec cited by Creager et al. (1973) and Cooper et al. (1979b) for the upper section of the Aleutian Basin turbidite unit the depth range for 90 percent of the VAMPs is 337.5-562.5 m with an average depth of 450 m and a maximum depth of 825 m. This is the depth at which the first indication of anomalous reflectors occurs

and the anomalies can continue for a considerable depth below the first occurrence, sometimes even into the underlying mudstone unit. The upper limit of the first occurrence of acoustic anomalies is important in that it may indicate a boundary through which trapped low-velocity fluids cannot migrate. The average velocity of the upper unit could be as high as 2000 m/sec (Cooper et al., 1979b) which would increase the minimum depth of VAMP occurrence to 450 m. Data from DSDP Site 190 shows the upper turbidite unit to be 375-m thick and it is suggested that this unit is thin in this area due to the basement topography. Therefore, in the more central regions of the basin it can be assumed that the upper unit could be of a thickness greater than 375 m. The data displayed in figure 10 indicates a definite boundary or upper limit to VAMP occurrence and the sediment characteristics of the upper diatomaceous turbidite unit may be such as to hinder upward hydrocarbon migration.

The areal extent of individual VAMPs appears to be limited. The average width of a VAMP is 1.3 km with a range of 0.5-3.75 km. Other anomalous areas range as wide as 15 km with the widest areas associated with the buried ridges of the basin. Our data indicate that the orientation of the crossing of the VAMPs does not significantly change the average width of these features suggesting that VAMPs are essentially circular in plan view and that each one exists independent of any others. Our attempts to correlate VAMP characteristics were unsuccessful which suggests that VAMPs occur as separate features although the process for the formation and timing is about the same. VAMPs, therefore, are probably separate pockets of gaseous sediment and hundreds of these pockets occur throughout the basin.

Arching of the reflectors overlying the VAMPs was first observed by Scholl and Cooper (1978) and was related to the possible presence of gas hydrates or to differential compaction over basement highs. While we cannot prove that their interpretation is incorrect, our data suggest that: 1) the arched reflectors above the VAMPs are continuous and undisturbed and do not show the anomalous features commonly associated with the VAMPs, such as phase inversion and high amplitude reflectors, and 2) although 58 percent of the VAMPs exhibited overlying arching reflectors only 28 percent were recorded over basement highs. We did find a few areas where the arching of overlying reflectors extended to the surface with as much as 2 meters of sea floor relief. We therefore suggest that another possible cause for arched reflectors may be the over-pressuring of the sediment above the VAMPs, causing the sediment to bow upward as the gas slowly migrates through the sediment.

Scholl and Cooper (1978) suggest that VAMPs occur around the edges of the basin where the sediment column is thinnest. Our data suggests that VAMPs occur in increasing numbers from north to south. The general trend in sediment thickness shows an increase from north to south (Marlow et al., 1979) suggesting that the availability of hydrocarbon producing material may increase with sediment thickness. Augmenting the sediment thickness in the south would be an increase in temperature due to the nearness of the heat producing source of the fossil island arc, Bowers Ridge.

The Aleutian Basin is a marginal basin of Paleogene age containing numerous basement ridges and thick sections of sediment between the ridges. The thickness of the sediment and the age of the lower section suggests that the generation of hydrocarbons is possible given that the necessary source beds exist. The bathymetry of the

basin shows a very gentle slope to the south and debris from the Beringian slope may be flowing out over the basin, perhaps as far south as Bowers Ridge. Mass wasting of the slope has been suggested as the dominant erosion process affecting the Beringian margin and Bowers Ridge (Carlson et al., 1986; Marlow et al., 1987; Karl et al., in press). On GLORIA sonographs extensive areas of sheet flow have been observed between the large canyons incising the Beringian slope and slump blocks kilometers wide and tens of kilometers long appear poised to slide from the slope (Carlson et al., 1987). Material of this volume sliding from the slope may attain velocities great enough to cover vast areas of the basin. The base of Bowers Ridge is significant in that it is the limit of the sloping basin and as such would be the absolute southern limit of sedimentation from the north. Further, sediment derived from the Aleutian Islands and northern slope of the Aleutian Arc just east of Bowers Ridge is transported to the north and west by a channel extending from Pochnoi Canyon. This sediment reaches another channel at the base of Bowers Ridge that has a general slope from east to west, around the ridge (fig. 2). The channel at the base of Bowers Ridge can be delineated not only from the bathymetry recorded during the Bering Sea cruise but also from GLORIA imagery which clearly depicts the channel as it follows the curvature of the ridge from east to west (Marlow et al., 1988). Deformation at the northern side of the channel indicates that major convergence probably occurred at Bowers Ridge during the late Mesozoic and early Tertiary and minor convergence from late Tertiary to as recently as late Cenozoic (Marlow et al., 1988). During the convergence, oceanic crust of the Aleutian Basin has been underthrust beneath Bowers Ridge and is probably responsible for the subduction-like bathymetry at the northern base of Bowers

Ridge. The underthrusting may also be a cause for increased temperature at depth in the southern area of the basin. It should be noted that VAMPs have also been discovered in Bowers Basin (Cooper et al., 1979b) where the major sediment sources have been the Aleutian Ridge, Bowers Ridge, and the settling of suspended material from the Bering Sea.

The increase in VAMPs and other acoustic anomalies near the base of Bowers ridge may be partially due to a change in sediment sources, a concentration of organic matter, and to increased heat flow near areas of subduction. Sediment from the Beringian slope may be rich in organic matter due to the high degree of upwelling. Sediment near the Aleutian slope may also be high in organic concentrations due to high productivity of the surface waters in this area. The increase in total sediment thickness to the south suggests that the general southward sloping of the Aleutian Basin is a feature that has persisted throughout much of the basin's history. The initial cause of the southward sloping could be either the load placed on the lithosphere by the Aleutian and Bowers Ridges or the overall bathymetry configuration created by subduction in the Aleutian Trench and, as stated above, from underthrusting at the northern base of Bowers Ridge. The southern area of the basin is also subjected to increased sedimentation due to the number of areas available to contribute sediment, including Bowers Ridge, the Aleutian Arc, and the Beringian slope, as well as normal pelagic sedimentation.

Hydrocarbon Potential

Conditions in the Aleutian Basin are favorable for the generation of hydrocarbons. Cooper et al. (1979b) discussed at length the hydrocarbon potential of the Aleutian Basin and determined that the possibility for hydrocarbon production is high for the following reasons: adequate thermal and sedimentation history, traps, source rocks, and reservoir beds. Cooper et al. (1979b) cite an average heat flow value of 1.44 ±0.22 $\mu cal/cm^2/sec$ in the Aleutian Basin. Although Schlanger and Combs (1975) suggest that this value is lower than that which is needed for hydrocarbon generation in marginal basins, it is not so low as to preclude the possibility of hydrocarbon generation. When all the known data are taken into account concerning temperature, age, and depth of burial as well as the sedimentation rate for Miocene through Holocene time (100 m/m.y.), Cooper et al. (1979b) suggest that hydrocarbon generation could occur in sediment as young as Miocene. The thickness (2-9 km), temperature, and age (late Mesozoic through Tertiary) of the sedimentary section above basement is certainly sufficient to have generated hydrocarbons. The basement topography of buried ridges and broad basement highs throughout the basin, together with the presence of faults, suggests that trapping mechanisms may exist for migrating hydrocarbons. The lower mudstone beds may serve as a source for hydrocarbon production (McIver, 1973), and the diatomaceous section immediately above as a reservoir.

Kvenvolden and Redden (1980) analyzed 2-m long gravity cores obtained from the Aleutian Basin for hydrocarbon gas concentrations. They found that, although overall gas concentrations are low, in the area of high VAMP concentration (fig. 2) the

volume of methane gas increased with depth in the cores (Table 4). Cores 2G1 and 6G2, collected directly above VAMPs, showed the down-core increase in methane to be particularly significant.

The acoustic anomalies surveyed in this study all lie within the upper-Cenozoic diatomaceous section suggesting that the hydrocarbons if present are trapped within this section and capped by the turbidite-bearing section above. The actual presence of methane in the upper few meters of sediment has been demonstrated by Kvenvolden and Redden (1980). All physical and acoustic evidence leads to the conclusion that hydrocarbons are present within the sediment of the Aleutian Basin; however, the economic importance remains unknown at this time.

CONCLUSIONS

Anomalous subbottom acoustic reflectors recorded during a 1986 GLORIA cruise suggest the presence of gaseous hydrocarbons in the subsurface. About 89 percent of the anomalous reflectors are interpreted as VAMPs, Velocity-AMPlitude anomalies, and exhibit reflector pulldown. Other acoustic anomalies include phase inversion, high-amplitude reflectors, diffraction hyperbola, and arching of the overlying reflectors. The size and distribution of the anomalous reflectors suggests that these are isolated pockets of gas that have migrated from a lower mudstone unit and are now trapped in a semi-indurated diatom-rich silty-clay unit that is capped by a diatomaceous silty-clay interbedded with terrigenous turbidites. The middle unit is permeable and porous and evidently forms an excellent trap for hydrocarbons, whereas, the overlying unit limits the upward migration of gaseous hydrocarbons.

Figure 4. Methane (C_1) Concentration in Cores from the Aleutian Basin.

(Kvenvolden and Redden, 1980)

Core No.	Interval (cm)	C_1 (nl/l interstitial water)
1G1	16 - 24	3500
	64 - 71	6100
2G1	2 - 10	1100
	34 - 44	5600
	61 - 71	12000
	87 - 97	21000
2G3	108 - 118	5900
3G1	2 - 12	900
	36 - 46	3300
	61 - 72	5500
	100 - 110	6700
	140 - 150	7100
	180 - 190	6900
	220 - 230	8600
4G1	2 - 12	300
	64 - 74	2500
	129 - 139	4500
	181 - 191	5400
6G2	0 - 10	2400
	60 - 70	5000
	120 - 130	5100
	167 - 177	11000
7G4	65 - 75	4700
8G2	1 - 11	500
	29 - 39	1600
	63 - 73	1600

VAMPs increase in concentration from north to south and may be related to differences in sediment thickness, source terrains, heat sources, and abundance of insection organic matter. Basement topography appears to play no roll in the concentration of the VAMPs, although other more extensive anomalous reflectors are found over the crests of buried basement ridges. Sediment in the northern areas of the basin is derived primarily from mass wasting of the Beringian slope and from a pelagic rain of sediment from surface waters. In the south, most sediment is derived from the Aleutian and Bowers Ridges and the pelagic "rain". Sediment from the northern side of the Aleutian Ridge flows into the basin via Pochnoi Canyon's main channel and its' tributaries, eventually reaching an area of the basin lying to the north of Bowers Ridge. A channel at the base of Bowers Ridge may further direct the westward transport of sediment. The general slope of the basin (about 0.05°) is to the south and west, also helping to confine sediment transport to these directions. During sea-level lowstands terrigenous sediment from Alaska and Siberia may have been the primary source of basin filling material. These materials may have been high in organic matter, further contributing to potential hydrocarbon source materials.

The cause for the arched reflectors overlying the VAMPs has been explained as possibly indicating the presence of gas hydrates or of differential compaction and faulting over basement highs. Detailed bathymetry from the present study shows that arching has occurred at the sea floor surface with as much as a few meters of vertical displacement taking place. Also noted in the data is the difference in the number of VAMPs with arching (58%) verses the number found over basement highs (28%). From this data we therefore suggest another possible explanation may be the over-

pressuring of the overlying sediment as gaseous hydrocarbons migrate from depth.

REFERENCES CITED

Carlson, P.R., Marlow, M.S., Rearic, D.M., Dadisman, S.V., and Parson, L.M., 1986, GLORIA side-scan imagery of the central Bering Sea: EOS, Transactions, American Geophysical Union, v. 67, n. 44, p. 1228-1229.

Carlson, P.R., Marlow, M.S., Rearic, D.M., and Parson, L.M., 1987, The GLORIA view of seafloor processes in Navarinsky and Pervenets Canyons, Bering Sea, Alaska: EOS, Transactions, American Geophysical Union, v. 68, n. 44, p. 1316.

Carlson, P.R., Marlow, M.S., Parson, L.M., and Somers, M.L., 1987, GLORIA investigation of the Exclusive Economic Zone in the deep Bering Sea; M/V Farnella cruise F2-86-BS: U.S. Geological Survey Open-File Report 87-72, 16 p.

Cooper, A.K., Marlow, M.S., Parker, A.W., and Childs, J.R., 1979a, Structure-contour map on acoustic basement in the Bering Sea: U.S. Geological Survey, Miscellaneous Field Studies Map MF-1165.

Cooper, A.K., Scholl, D.W., Marlow, M.S., Childs, J.R., Redden, G.D., Kvenvolden, K.A., and Stevenson, A.J., 1979b, Hydrocarbon potential of the Aleutian Basin, Bering Sea: AAPG Bulletin, v. 63, n. 11, p. 2070-2087.

Creager, J.S., Scholl, D.W., et al., 1973, Initial reports of the Deep Sea Drilling Project (Vol. 19): Washington D.C., U.S. Government Printing Office, 913 p.

Hall, R.K., Karl, H.A., Carlson, P.R., Cooper, A.K., Gardner, J.V., Hunter, R.E., Marlow, M.S., and Stevenson, A.J., in press, Bathymetric map of the Aleutian Basin and Bowers Basin east of the U.S.-U.S.S.R. 1867 Convention Line, Bering Sea: U.S. Geological Survey Open-File Report, 10 p.

Karl, H.A., et al., in press, GLORIA view of sedimentation styles and patterns across the Aleutian Island Arc - outer oceanic plate to backarc basin of the Bering Sea: 28th International Geological Congress, Washington D.C., July, 1989, 3 p.

Kvenvolden, K.A., and Redden, G.D., 1980, Hydrocarbon gas in sediment from the shelf, slope, and basin of the Bering Sea: Geochimica et Cosmochimica Acta, v. 44, p. 1145-1150.

Marlow, M.S., Carlson, P.R., Dadisman, S.V., Rearic, D.M., Maple, E.J., and Parson, L.M., 1987, GLORIA side-scan and geophysical surveys of the central Bering Sea in 1986: Geologic Studies in Alaska by the U.S. Geological Survey During 1986, U.S. Geological Survey Circular 998, p. 152-156.

Marlow, M.S., Cooper, A.K., Dadisman, S.V., Carlson, P.W., Geist, E., and Parson, L.M., 1988, Recent deformation along Bowers Ridge, Bering Sea: evidence from GLORIA images and seismic-reflection data: Proceedings, Annual Meeting of Geological Society of America, p. .

Marlow, M.S., Cooper, A.K., Parker, A.W., and Childs, J.R., 1979, Isopach map of strata above acoustic basement in the Bering Sea: U.S. Geological Survey, Miscellaneous Field Studies Map MF-1164.

McIver, R.D., 1973, Hydrocarbons in canned muds from sites 185, 186, 189, and 191: in Deep Sea Drilling Project Initial Reports (Vol. 19), Washington D.C., U.S. Government Printing Office, v. 19, p. 875-878.

Rowland, R.W., Goud, M.R., and Mcgregor, B.A., 1983, The U.S. Exclusive Economic Zone - a summary of its' geology, exploration, and resource potential: U.S. Geological Survey Circular 912, 29 p.

Schlanger, S.O., and Combs, J., 1975, Hydrocarbon potential of marginal basins bounded by an island arc: Geology, v. 3, n. 7, p. 397-400.

Scholl, D. W., and Creager, J.S., 1973, Geologic synthesis of Leg 19 (DSDP) results: Far North Pacific, Aleutian Ridge and Bering Sea, in Deep Sea Drilling Project Initial Reports (Vol. 19), Washington D.C., U.S. Government Printing Office, v. 19, p. 897-913.

Scholl, D.W., and Cooper, A.K., 1978, VAMPS - Possible hydrocarbon-bearing structures in the Bering Sea basin: AAPG Bulletin, v. 62, n. 12, p. 2481-2488.

APPENDIX I

VAMP Attributes								
Latitude	Longitude	Width of VAMP (km)	Depth to VAMP (msec)	Maximum Amplitude (msec)	Depth to Arching (msec)	PI	HAR	DH/BT
57.76125 N	177.86615 W	1.25	500	20	350	X		
58.23570 N	179.05370 E	1.00	550	20	400	X		
58.29620 N	178.87855 E	0.75	500	20		X		
58.27580 N	178.95590 E	0.50	850	20		X		X
58.43140 N	178.50780 E	1.00	700	30				
58.57230 N	178.10201 E	1.00	650	20			X	
58.74130 N	177.59331 E	1.00	950	20	200	X		
58.41755 N	177.60080 E	1.75	650	50	600	X		X
58.34450 N	177.83650 E	1.75	520	50	350	X		
58.18020 N	178.27355 E	1.50	570	40		X		
58.14130 N	178.37910 E	2.00	520	70	370	X		X
58.00990 N	178.79430 E	1.25	650	50		X		X
57.88030 N	179.20030 E	0.75	750	50		X		
57.75810 N	179.50610 E	2.00	550	20	480	X		
57.07440 N	179.13499 W	1.50	470	50	450	X		X
57.62160 N	178.96030 E	2.00	770	50	450	X	X	
57.64355 N	178.89435 E	2.00	460	40	450	X		
57.78360 N	178.53360 E	2.75	570	50	370			X
58.33295 N	176.91845 E	1.00	700	20	400		X	
57.85370 N	177.38170 E	1.50	600	40	400		X	
57.76185 N	177.68460 E	2.50	500	40	420	X	X	
57.68080 N	177.93925 E	1.50	780	30			X	
57.16510 N	179.34480 E	2.25	450	50	300	X		
57.14830 N	179.38546 E	1.50	500	60		X		X
56.88790 N	179.85150 W	1.50	550	30	520			X
56.66985 N	179.27510 W	1.75	550	50	250	X		
56.38900 N	178.73940 W	2.00	450	40	200	X		
56.36030 N	178.77560 W	2.25	450	60	220	X		X
56.28860 N	178.87041 W	1.50	450	20	280	X		
56.27550 N	178.88831 W	1.50	650	30		X		X
56.35185 N	179.33565 W	2.00	450	20	300	X		
56.42530 N	179.54111 W	1.50	450	20	200	X	X	
56.93560 N	179.10705 E	2.00	600	40		X		
56.95180 N	179.06040 E	2.00	550	60		X		
56.96930 N	179.01010 E	1.00	650	30		X		
57.54560 N	177.38251 E	0.75	500	20	380	X		
57.56530 N	177.32595 E	0.75	450	20	300	X		
57.72775 N	176.85155 E	0.75	650	20		X		
57.80930 N	176.60831 E	0.75	550	20		X		
57.83880 N	176.51230 E	0.75	500	20		X		
57.98105 N	176.03630 E	1.25	550	20	400	X	X	

VAMP Attributes								
Latitude	Longitude	Width of VAMP (km)	Depth to VAMP (msec)	Maximum Amplitude (msec)	Depth to Arching (msec)	PI	HAR	DH/BT
57.75630 N	175.75639 E	1.50	800	20	550			
57.70910 N	175.92281 E	1.50	600	20	550	X	X	
57.63420 N	176.19300 E	1.50	650	20	600			X
57.57355 N	176.39840 E	1.75	450	30	400	X		
57.39940 N	176.87360 E	1.50	450	40		X		
57.35610 N	176.99310 E	1.00	650	20	400	X		X
57.29780 N	177.15630 E	1.25	700	30				
57.26385 N	177.25611 E	0.75	950	10	650	X	X	
57.11985 N	177.73405 E	2.50	600	20	200	X	X	
57.06810 N	177.87601 E	1.75	500	30	250	X		
57.01230 N	178.02740 E	2.00	600	50	450	X		X
56.98090 N	178.10995 E	1.25	800	30				X
56.71540 N	178.83389 E	1.00	650	20		X		
56.43480 N	179.59180 E	1.25	750	20	300	X		
56.25910 N	179.92731 W	2.00	550	50	500	X		
56.19645 N	179.77240 W	1.50	700	30				
55.86520 N	179.75321 W	1.50	500	40	450	X		
55.90180 N	179.84140 W	1.50	650	30				
56.03480 N	179.82640 E	1.25	700	20				
56.08160 N	179.70081 E	1.75	700	30		X		
56.13680 N	179.52710 E	1.25	700	10	450	X		
56.15480 N	179.46930 E	2.00	450	30	400	X		X
56.17560 N	179.40480 E	1.50	600	10		X		
56.23410 N	179.23129 E	1.00	700	10				
56.27760 N	179.10510 E	1.25	700	20				
56.29800 N	179.04761 E	1.50	600	10				
56.33095 N	178.95725 E	2.25	750	30				
56.41025 N	178.75180 E	1.25	700	20			X	
56.53350 N	178.43230 E	2.50	450	60	350	X	X	X
56.70210 N	177.99030 E	2.00	500	30	300	X		
56.71260 N	177.96111 E	1.50	550	30		X		
56.74460 N	177.87131 E	1.00	600	10				
56.78780 N	177.74695 E	1.25	650	30		X		
56.79950 N	177.71330 E	1.50	550	20		X		
56.81580 N	177.66811 E	1.00	600	20	400	X		
56.86210 N	177.54080 E	1.25	550	30				
56.90730 N	177.41029 E	1.75	700	30		X		
56.98425 N	177.19430 E	1.25	500	20		X		
57.02130 N	177.09140 E	1.25	650	20	300	X		X
57.09160 N	176.89281 E	0.75	900	10		X		X
57.11010 N	176.83910 E	1.25	500	20	200	X		X

VAMP Attributes								
Latitude	Longitude	Width of VAMP (km)	Depth to VAMP (msec)	Maximum Amplitude (msec)	Depth to Arching (msec)	PI	HAR	DH/BT
57.12080 N	176.80830 E	0.75	550	20	300	X	X	X
57.20330 N	176.56129 E	1.00	600	20	400		X	X
57.23390 N	176.46989 E	0.75	750	20				
57.24730 N	176.43159 E	1.00	450	20	350	X		
57.27580 N	176.34850 E	1.50	600	10	300	X		
57.32790 N	176.19825 E	1.50	700	10	500		X	
57.36460 N	176.07829 E	1.75	500	20	300	X		
57.42830 N	175.86790 E	1.00	500	20	400	X		
57.48515 N	175.69670 E	1.00	1000	20	400			
57.51380 N	175.60950 E	1.50	900	10	650			
57.58165 N	175.39600 E	1.00	700	10	400			
57.60500 N	175.32230 E	1.00	700	20			X	
57.44595 N	174.99810 E	1.50	650	10			X	
57.27965 N	175.33661 E	1.25	800	20	500	X		
57.17300 N	175.68460 E	1.25	500	10		X		
57.13315 N	175.80600 E	1.50	500	20	350	X	X	
57.04625 N	176.05246 E	1.00	550	10	500	X		
56.88280 N	176.54980 E	1.25	450	20	300	X		
56.83730 N	176.70180 E	1.00	550	20		X		
56.74960 N	176.96080 E	1.50	550	20	200	X	X	
56.73530 N	176.99960 E	1.00	600	20	400	X	X	X
56.70480 N	177.08560 E	1.25	750	10			X	
56.57710 N	177.44930 E	1.50	950	20		X		
56.56805 N	177.47535 E	1.00	950	20		X		
56.55825 N	177.50506 E	1.25	1000	20		X		
56.50380 N	177.67180 E	2.00	600	30		X		
56.44830 N	177.82660 E	1.50	500	30		X		
56.40910 N	177.92530 E	1.75	570	30	400	X		
56.37520 N	178.01080 E	1.25	550	20	400	X	X	
56.33240 N	178.11861 E	1.50	500	20	450	X		
56.31980 N	178.15240 E	1.25	550	20	400	X		
56.28150 N	178.25560 E	1.50	600	20		X		
56.18230 N	178.55409 E	0.75	650	10		X		
56.13360 N	178.70430 E	0.75	550	10		X		
56.02455 N	179.02321 E	1.50	600	20	500	X		
55.99660 N	179.09860 E	1.25	500	20		X		
55.86630 N	179.42860 E	1.00	550	20	450	X		
55.80035 N	179.59274 E	1.00	550	20		X		
55.73690 N	179.74420 E	1.00	550	30		X		
55.70330 N	179.83416 E	1.25	550	20	400	X		
55.50560 N	179.93581 W	2.50	550	30	300	X		

VAMP Attributes								
Latitude	Longitude	Width of VAMP (km)	Depth to VAMP (msec)	Maximum Amplitude (msec)	Depth to Arching (msec)	PI	HAR	DH/BT
55.38880 N	179.92480 E	1.25	650	20		X		
55.35790 N	179.85159 E	1.25	650	40	400			X
55.39655 N	179.75431 E	1.00	900	10	400	X		
55.46430 N	179.57820 E	1.50	500	50	300	X	X	
55.48480 N	179.52185 E	0.75	850	10		X		
55.53910 N	179.37860 E	1.25	1100	10	800	X		
55.58880 N	179.24651 E	1.00	550	20	400	X	X	
55.73860 N	178.87900 E	1.00	500	30	400	X		
55.93130 N	178.35834 E	1.00	600	20		X		
55.95360 N	178.29380 E	1.00	500	10		X		
56.04390 N	178.04225 E	1.00	450	20		X		
56.06380 N	177.98990 E	1.00	500	20		X		
56.09030 N	177.91901 E	1.00	450	20		X		
56.13415 N	177.80210 E	1.25	700	10	300			
56.18660 N	177.66451 E	1.00	650	10	450		X	
56.20410 N	177.61835 E	1.00	450	30		X		
56.22180 N	177.57230 E	1.50	600	30		X		
56.24805 N	177.50470 E	1.50	600	40	400	X		
56.29280 N	177.38930 E	1.25	650	30	450	X	X	
56.31880 N	177.32040 E	1.00	700	10		X		
56.56010 N	176.57895 E	1.00	500	30	350	X		
56.58630 N	176.50150 E	1.00	500	10	350	X		
56.60380 N	176.44980 E	0.50	650	10	450	X		
56.61910 N	176.40500 E	1.00	550	30	350	X		
56.63140 N	176.36830 E	1.00	550	30	350	X		
56.66430 N	176.27209 E	1.50	600	20	250	X		
56.69045 N	176.19440 E	2.00	550	30	300	X		X
56.71500 N	176.12040 E	1.75	550	30	350	X		X
56.91380 N	175.52530 E	1.00	500	30	350	X		X
56.96580 N	175.37910 E	1.50	500	30	300	X		
57.11210 N	174.93559 E	1.00	500	30	300	X	X	
57.18550 N	174.71280 E	1.00	500	10		X		
57.19590 N	174.68130 E	1.00	550	30	400	X		
57.17630 N	174.57930 E	1.25	500	20	350	X	X	
57.03090 N	174.37830 E	1.00	600	10		X		
56.95680 N	174.48579 E	1.25	500	20		X		
56.83415 N	174.82795 E	0.75	500	10	400	X		
56.73360 N	175.13440 E	1.25	600	20		X	X	X
56.70210 N	175.23779 E	1.25	650	10		X		
56.64370 N	175.42500 E	1.00	600	10	300	X		
56.41520 N	176.10871 E	1.00	550	10		X		X

VAMP Attributes								
Latitude	Longitude	Width of VAMP (km)	Depth to VAMP (msec)	Maximum Amplitude (msec)	Depth to Arching (msec)	PI	HAR	DH/BT
56.37810 N	176.22050 E	1.00	650	20				X
56.27830 N	176.52100 E	1.00	500	20	350	X	X	
56.26910 N	176.54880 E	1.00	600	20	350	X		
56.25680 N	176.58411 E	1.00	650	20			X	
56.23280 N	176.65440 E	1.00	800	10	300			
56.18350 N	176.79700 E	1.25	500	10	350	X		
56.14600 N	176.90615 E	1.50	550	10	400	X		X
56.01595 N	177.27560 E	1.00	800	20	350			
55.79985 N	177.86155 E	1.00	650	30	350	X	X	
55.76710 N	177.93736 E	1.00	550	20		X		
55.65380 N	178.22400 E	1.25	600	20	300	X		
55.66020 N	177.34580 E	0.75	850	10				
55.67335 N	177.31029 E	1.00	600	20	350	X		
55.69485 N	177.25300 E	1.00	950	10				
55.76900 N	177.05640 E	0.75	550	10	400	X		
55.96735 N	176.53029 E	0.75	550	40	300	X		X
55.99570 N	176.44230 E	1.00	650	20	400	X		
56.01100 N	176.39510 E	0.75	650	10	400	X		
56.05060 N	176.27341 E	0.50	650	20	400	X		
56.06315 N	176.23395 E	1.25	550	20	350	X	X	
56.07545 N	176.19735 E	1.25	500	30		X	X	
56.08800 N	176.15880 E	0.75	750	40	350	X		
56.09845 N	176.12675 E	0.75	750	30				
56.11070 N	176.09099 E	1.00	650	40				
56.24420 N	175.70160 E	1.00	1000	20				
56.30785 N	175.51255 E	1.00	700	20	450	X		
56.33540 N	175.43260 E	1.50	650	30	300	X		
56.64725 N	174.41449 E	1.00	800	10	400	X		X
56.72440 N	174.16310 E	0.75	600	20	400	X		X
56.62560 N	173.80090 E	1.00	750	10		X	X	X
56.49300 N	173.97549 E	1.50	700	30				
56.48180 N	174.01010 E	1.25	600	30				
56.45622 N	174.09252 E	1.00	750	30		X		
56.44420 N	174.13236 E	1.50	650	30		X		
56.42490 N	174.19745 E	1.00	800	20	500	X		
56.25760 N	174.73640 E	1.00	550	10		X		
56.16295 N	175.01255 E	0.75	550	10	300	X		
56.14670 N	175.05909 E	1.25	500	10		X	X	
56.12580 N	175.11929 E	1.50	500	20	350	X	X	X
56.05275 N	175.32756 E	1.00	550	30	300	X		
56.02780 N	175.39776 E	1.00	650	30	250			

VAMP Attributes								
Latitude	Longitude	Width of VAMP (km)	Depth to VAMP (msec)	Maximum Amplitude (msec)	Depth to Arching (msec)	PI	HAR	DH/BT
56.01230 N	175.44090 E	1.25	500	20	300	X	X	X
55.96260 N	175.57401 E	0.75	700	10				
55.94550 N	175.61929 E	0.75	470	10		X		
55.84955 N	175.87136 E	0.50	700	20	400			
55.83750 N	175.90530 E	0.75	650	20	300			
55.82430 N	175.94240 E	1.00	550	30	250	X		X
55.76780 N	176.11110 E	1.25	600	30	350			
55.74460 N	176.18410 E	1.00	550	20	250	X		
55.71310 N	176.28450 E	1.00	800	20	400			
55.48625 N	176.04400 E	1.00	850	20		X		
55.50595 N	175.98506 E	1.00	650	10		X		
55.57830 N	175.79830 E	1.00	850	20	300	X		
55.61900 N	175.68845 E	1.50	450	30	300	X		
55.72580 N	175.38910 E	1.00	550	20		X		X
55.76835 N	175.28035 E	1.50	500	20		X		
55.79325 N	175.21521 E	1.00	600	20		X		
55.81530 N	175.15631 E	1.25	650	10		X		
55.83060 N	175.11590 E	1.50	600	10	450	X		
55.84300 N	175.08251 E	1.50	650	20	450	X		X
55.91865 N	174.87670 E	1.50	550	10	450			
55.95730 N	174.75960 E	1.75	550	20	450	X	X	X
55.97910 N	174.69150 E	1.50	550	30		X	X	X
55.99950 N	174.62856 E	2.50	650	30	150	X	X	X
56.03170 N	174.52945 E	2.25	450	20	150	X		X
56.21315 N	173.94296 E	1.50	500	10	250	X		
56.22870 N	173.89085 E	2.50	500	10	350	X		
56.24810 N	173.82325 E	2.25	450	20	200	X		
56.29300 N	173.67000 E	1.50	500	20		X		
56.31430 N	173.59720 E	3.75	450	20		X		
56.38875 N	173.53770 E	1.50	450	10	100	X	X	
56.39060 N	174.72740 E	1.75	700	10				
56.45360 N	174.88350 E	1.50	800	10		X		
56.56355 N	175.21670 E	1.50	650	20		X		X
56.56010 N	175.36530 E	1.50	500	30	250	X		
56.55790 N	175.45731 E	1.25	500	20	200	X		
56.25370 N	175.97660 E	1.00	600	20		X		
56.27920 N	176.09105 E	1.50	550	40		X		X
56.28530 N	176.11549 E	1.00	700	10				
56.31810 N	176.26326 E	2.00	550	20		X		X
57.13200 N	177.75100 E	1.50	700	10	250		X	X
57.15700 N	177.78200 E	1.50	500	20	350	X		X

APPENDIX II

Wide Anomolous Reflector Zones

Start		End		Depth	
Latitude	Longitude	Latitude	Longitude	(msec)	Description
57.67410 N	179.73560 E	57.29270 N	179.25404 W	1000-1100	7 zones of arching reflectors.
58.34450 N	176.38080 E	58.32560 N	176.23735 E	500	possible gas-charged sediment.
56.72810 N	179.42349 W	56.70150 N	179.35480 W	500	possible gas-charged sediment.
56.82080 N	175.80209 E	56.85830 N	175.68980 E	500-700	bright, sub-horizontal reflectors.
55.45600 N	177.93430 E	55.49310 N	177.83231 E	450-650	bright, sub-horizontal, discordant reflectors.
56.35460 N	175.37630 E	56.38460 N	175.29260 E	450-650	zone of inversion.
56.46840 N	175.03090 E	56.49630 N	174.93860 E	400-750	zone of inversion.
56.33860 N	174.48430 E	56.30805 N	174.58080 E	450-550	sub-horizontal, discordant reflectors.
56.24130 N	174.78281 E	56.21670 N	174.85581 E	450-700	sub-horizontal, discordant bright spots with arching at a depth of 200 msec.
56.14380 N	174.17439 E	56.18530 N	174.03690 E	600-850	high-amplitude reflectors suggesting possible gas-charged sediment.
56.48210 N	174.95129 E	56.54030 N	175.09360 E	400-800	possible gas-charged sediment over basement ridge.
56.53535 N	175.72141 E	56.45810 N	175.73911 E	50-90	interference zone over basement ridge.
56.37130 N	175.75790 E	56.32780 N	175.76801 E	350-500	sub-horizontal, bright reflectors over basement ridge.
57.25100 N	177.85000 E	57.36000 N	177.93700 E	100-800	sub-horizontal, bright reflectors over basement ridge.